THE JOURNAL OF PHYSICAL CHEMISTRY B

Article

pubs.acs.org/JPCB

Computational Analysis of Methyl Transfer Reactions in Dengue Virus Methyltransferase

Tobias Schmidt,[†] Torsten Schwede,[†] and Markus Meuwly*[,‡]

[‡]Department of Chemistry, University of Basel, Klingelbergstrasse 80, 4056Basel, Switzerland

[†]SIB Swiss Institute of Bioinformatics, Basel, Switzerland Biozentrum, University of Basel, Klingelbergstrasse 50/70, 4056 Basel, Switzerland

ABSTRACT: S-Adenosyl-L-methionine (SAM) dependent methyltransferases (MTases) play crucial roles in many biological processes. The MTase of the dengue virus is of particular interest for the development of antiviral drugs against flaviviruses. It catalyzes two distinct methylation reactions at the N7 and the 2′O position of the viral RNA cap structure. Based on density functional theory (DFT) electronic structure calculations, the molecular basis of the underlying chemical reactions involved in the N7 and the 2′O methyl transfer reactions of this enzyme were investigated using model systems. Calculations in the condensed phase show that both reactions are exergonic with significant activation barriers of 13.7 and 17.6 kcal/mol and stable product states, stabilized by 23.5 and 16.9 kcal/mol compared to the reactant states for the N7 and the 2′O reaction, respectively. We find that the reaction rate for the 2′O reaction is significantly enhanced in the presence of the native proton acceptor group, which lowers the activation barrier in the catalyzed reaction by 3.8 kcal/mol compared to the uncatalyzed reaction in aqueous solution. Furthermore, the 2′O reaction involves a methyl and a proton transfer reaction. Our results suggest that these two reactions occur in a concerted fashion in which the methyl group and the proton are transferred simultaneously. From a therapeutic viewpoint, SAM analogues stable under physiological conditions are particularly relevant. One such compound in MeAzaSAM, an isostructural mimic of SAM, for which the present calculations suggest that the methyl transfer reaction is unlikely to occur under biologically relevant conditions.

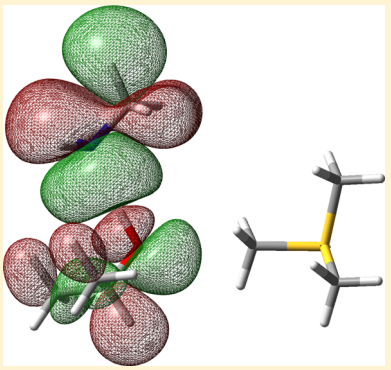

INTRODUCTION

Methyl transfer reactions play crucial roles in many biological processes including metabolism, signaling, regulation, and molecular recognition. The transfer of methyl groups onto particular substrates is catalyzed by methyltransferases (MTases). Overall, more than 150 different reactions are catalyzed by various MTases with diverse methylation targets including small molecules, proteins, nucleic acids, and glycans. Methyl group acceptor atoms can be nitrogen, oxygen, carbon, sulfur, or halides.[1]

Although several MTase classes are known, most reactions are catalyzed by S-adenosyl-L-methionine- (SAM) dependent MTases where SAM acts as a methyl group donor to methylate the substrate.[2] Other methyl donors include tetrahydrofolic acid and betaine, but biologically, SAM is largely preferred due to the associated highly favorable reaction energetics.[3]

SAM is a high energy compound in which the methyl group, activated by a sulfonium center,[4] induces a partial positive charge on the neighboring methyl group.[1] Although the methyl transfer reaction is thermodynamically highly favorable with a free energy gain of ∼17 kcal/mol,[2] the reaction is often kinetically inhibited and thus enzymatic catalysis is often required. Generally, the methylation reaction is assumed to occur in an S_N2-type reaction as shown in Figure 1.

Enzymatic catalysis largely facilitates this reaction through two different effects: first, by correctly arranging the two substrates in close proximity and thereby increasing the effective concentration of the reaction partners;[5] second, through activation of the attacking nucleophile which can occur by abstraction of a proton or by alignment of a nucleophile lone pair, which is of particular importance in case of a protonated nucleophile where the overall reaction represents a substitution of a hydrogen atom by a methyl group.[6,7]

Since MTases play key roles in many biological processes, they are potential drug targets for a wide variety of diseases, with applications against cancer,[8] neurodegeneration,[9] viral infections,[10] and many others. One SAM-dependent MTase of particular interest for the development of antiviral drugs against flaviviruses is the MTase located at the N-terminal domain of the nonstructural protein 5 (NS5) of the dengue virus.[11] This MTase is essential in the maturation process of the viral genome in which a type 1 cap structure is added at the 5′-end of the viral RNA.[12] This cap structure is vital for viral replication, since it ensures RNA stability by protecting against RNases and it enhances recognition by the ribosomes.[13,14] The capping process includes two methylation reactions: first, at the cap guanosine amino group in the 7 position (N7) and second,

Received: March 22, 2014
Revised: May 7, 2014

   dx.doi.org/10.1021/jp5028564 | J. Phys. Chem. B XXXX, XXX, XXX−XXX

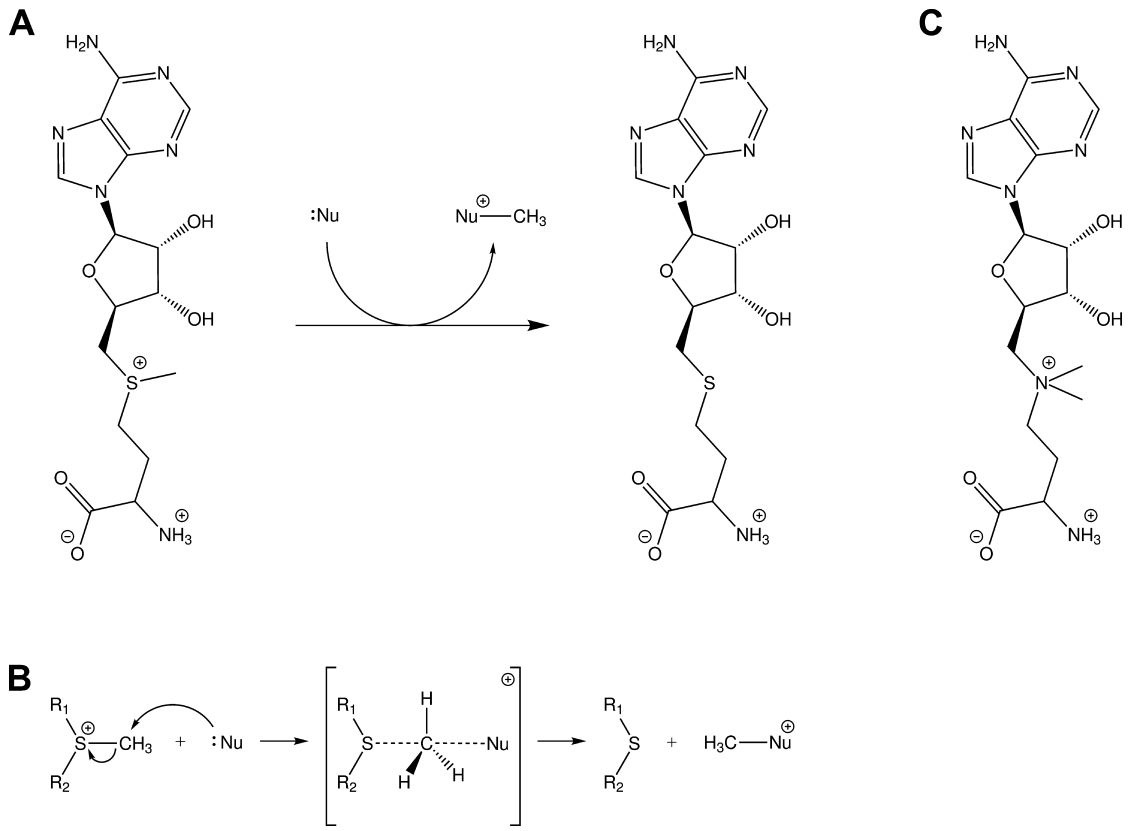

Figure 1. Methylation of a nucleophile (Nu) by SAM-dependent methyltransferase. (A) Overview of the reaction in which the methyl donor SAM is converted to the product S-adenosyl-L-homocysteine (SAH) yielding a methylated nucleophile (Nu-CH_3). (B) Detailed representation of the reaction mechanism of the nucleophilic attack in which R_1 and R_2 represent the adenosyl and aminobutyryl moieties. (C) Chemical structure of the SAM analogue MeAzaSAM.

at the ribose 2′-hydroxy group (2′O) of the first RNA nucleotide. Both methylation reactions are catalyzed by NS5MTase.[11,15]

Although flaviviral methyltransferases are attractive drug targets,[16,17] little is known about the mechanism underlying their function. The enzyme is known to catalyze two distinct reactions on an RNA cap structure with a specific sequence,[14,18,19] but so far a detailed structural and mechanistic understanding of these reactions is largely missing. Thus, to obtain more insight into the underlying chemical reactions involved in the guanosine N7 and the adenosine 2′O methyl transfer reactions, DFT electronic structure calculations were performed on model systems mimicking the biological reactions.

MATERIALS AND METHODS

Model Systems. Three different model systems were considered to study the reaction energetics on simplified systems. One for the N7 reaction and two for the 2′O reaction where the proton acceptor was either a lysine-like molecule or a water molecule. The initial geometry was based on an atomistic model derived from the X-ray structures of the homologue E. cuniculi cap MTase Ecm1[5] and the vaccinia virus VP39 MTase[6] for the N7 and the 2′O reaction, respectively. The model systems are shown in Figure 2.

The model for the N7 reaction consists of two groups: (1) a model of the methyl donor SAM, which is truncated one carbon away from the reactive sulfur atom; (2) an *N*-methylimidazole mimicking the methyl acceptor guanosine.

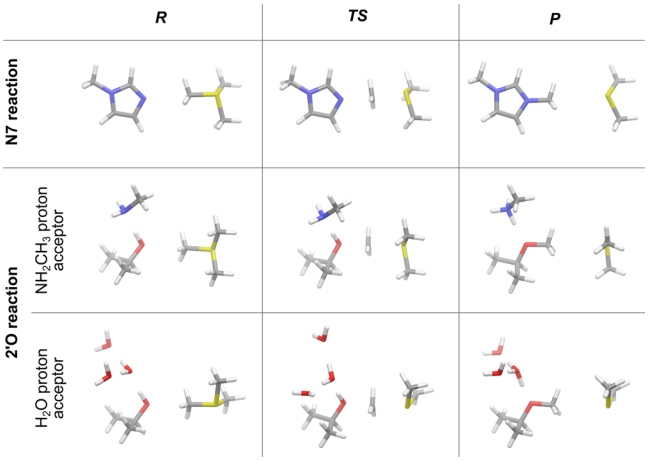

Figure 2. Optimized structures of reactants (R), products (P), and transition states (TS) obtained by DFT calculations for the three different model systems: (top) N7 reaction, (middle) 2′O reaction with a NH_2CH_3 molecule to act as proton acceptor, and (bottom) 2′O reaction with a water molecule as proton acceptor.

For this reaction, no proton needs to be abstracted. Thus, those two groups are sufficient to describe the reaction. The geometry optimized structures of this model are shown in the top panel of Figure 2.

The model for the 2′O reaction consists of the following three groups: (1) the methyl donor SAM as described above for the N7 reaction; (2) the methyl acceptor ribose moiety, which is truncated two carbon atoms away from the reactive 2′

dx.doi.org/10.1021/jp5028564 | J. Phys. Chem. B XXXX, XXX, XXX−XXX

hydroxy group; (3) the side chain of Lys181, truncated one carbon atom away from the Nζ, which acts as a proton acceptor. The geometry optimized structures of this model are shown in the middle panel of Figure 2.

A third model was designed to investigate the uncatalyzed 2′O reaction. It is identical to that for the catalyzed 2′O reaction, except that the proton acceptor moiety is replaced by a water molecule that accepts the transferred proton. To stabilize this water molecule, two additional water molecules were added, which are hydrogen bonded to the active water but do not directly participate in the reaction. The geometry optimized structures of this model are shown in the bottom panel of Figure 2.

Model systems for the SAM analogue MeAzaSAM were generated from the optimized geometries of the SAM model systems in the product and the reactant state by manual replacement of the sulfur atom by a nitrogen atom and addition of a methyl group. MeAzaSAM systems were subsequently energy minimized as described below.

Electronic Structure Calculations. All electronic structure calculations were performed with Gaussian03[20] using the B3LYP[21] density functional theory method and the 6-311++G(d,p) basis set.[22] A similar level of theory was already employed in studying the Menshutkin reaction.[23] Solvation effects were included during both optimization and energy calculations based on the C-PCM implicit solvent model.[24] For all model systems, the reactant and the product complexes were fully optimized in implicit solvent. Subsequently, using the obtained structures, transition state optimization with QST3[25] was carried out. During all optimizations, all atoms were free to move. For all fully optimized structures, vibrational analyses were performed at the same level of theory in order to confirm the nature of the stationary points and to compute thermal corrections to the Gibbs free energy which include translational, rotational, and vibrational contributions. From the obtained energies, a free energy profile for the reaction was calculated and point charges were computed based on a natural bond orbital (NBO) analysis.[26]

Two-dimensional potential energy landscapes were computed for the model systems. Enthalpies of partially optimized structures were computed based on a two-dimensional linear scan along the following reaction coordinates: (1) distance between acceptor atom and transferring methyl group (d_3 in Figure 3), (2) distance between acceptor and donor atom (d_2 in Figure 3). For each combination of reaction coordinates, the hydrogen atoms of the transferred methyl group were fully minimized while keeping the rest of the system rigid. Optimizations and energy calculations were performed as described previously.

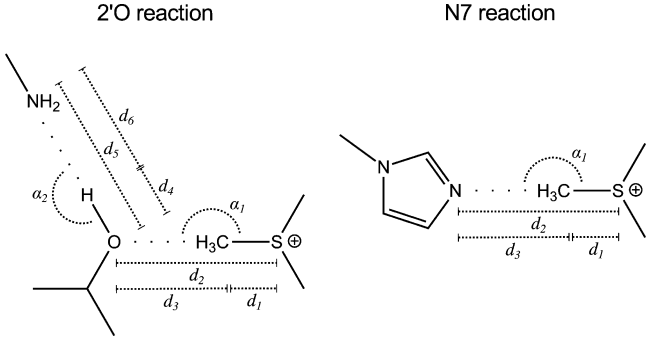

Figure 3. Schematic representation of the model systems for the 2′O and the N7 reaction. All reported distances and angles are indicated with italic labels. For the 2′O reaction, only the system with a NH_2CH_3 molecule as proton acceptor is shown since all geometric parameters are directly transferable.

Potential energy profiles for the proton transfer occurring during the 2′O reaction were calculated for the reactant state as well as the product state, based on a linear scan of the distance between the transferred proton of the 2′O hydroxy group and the Nζ of the lysine model moiety (d_6 in Figure 3). For the reactant state, the methyl group was bound to the SAM model compound, whereas for the product state, the methyl group was bound to the ribose moiety.

RESULTS

Reaction Geometry. In this study, model systems were used to study the methyl transfer reaction catalyzed by flaviviral methyltransferases using quantum chemical calculations. Model systems were designed for the 2′O and for the N7 reaction as described in Materials and Methods.

Figure 2 shows the optimized structures of all model systems for the reactant state (left row), the transition state (middle row), and the product state (right row). In all reactions, the methyl groups are transferred in a S_N2-type nucleophilic substitution reaction, where the lone pair of the acceptor group attacks the positively charged methyl group. This reaction involves an inversion of the methyl group with a planar methyl conformation in the transition state. In all reactions, a nearly linear arrangement between the donor, the transferring methyl group, and the acceptor was observed. Geometric parameters were extracted from the optimized structures as shown in Figure 3 with the values given in Tables 1 and 2 for the 2′O and the N7 model systems, respectively.

The distance between the methyl donor and acceptor atoms (d_2) shows similar behavior for all reactions. Starting from the reactant complex, in the transition state d_2 contracts by 0.5 and 0.4 Å for the N7 and the 2′O reaction, respectively. In comparison to the reactant state, d_2 in the product state is significantly increased by 0.5 and 0.65 Å for the N7 and the 2′O reactions, respectively. Thus, a significant compression of the structure in the transition state is observed which facilitates the reaction by lowering the energy barrier.

For both models of the 2′O reactions, the methyl group is transferred onto a hydroxy moiety, yielding a methoxy group as the result of the reaction. Since a protonated methoxy moiety is unstable (as discussed below), the proton needs to be abstracted by a proton acceptor. In the protein environment, this is performed by the Nζ atom of Lys181 which was shown to be present in a deprotonated state.[27,28] In the uncatalyzed reaction, however, this would be performed by a water molecule. The geometry of both model systems for the 2′O reaction are very similar for the reactant and the transition state. For the product state, however, the largest differences can be observed. For the uncatalyzed reaction, the distance between the methyl donor and acceptor (d_2) is decreased by 0.18 Å and the distance between the proton donor and acceptor (d_5) is reduced by 0.25 Å which leads to a smaller distance between the proton donor and the transferred hydrogen atom (d_4), reduced by 0.23 Å. Thus, the transferred hydrogen atom is more strongly bound to the methoxy group which indicates that the water molecule is a worse proton acceptor compared to the model of the lysine. This effect is even stronger when the two additional water molecules are removed from the model

dx.doi.org/10.1021/jp5028564 | J. Phys. Chem. B XXXX, XXX, XXX−XXX

Table 1. Geometric parameters obtained from minimized structures for model systems of the 2′O reaction (Figure 3)[a]

	NH_2CH_3 proton acceptor			H_2O proton acceptor		
	reactant complex	transition state	product complex	reactant complex	transition state	product complex
d_1 (Å)	1.82	2.39	4.00	1.82	2.39	3.82
d_2 (Å)	4.78	4.36	5.43	4.82	4.36	5.25
d_3 (Å)	2.96	1.97	1.43	2.99	1.97	1.44
d_4 (Å)	0.99	1.04	1.72	0.98	1.00	1.49
d_5 (Å)	2.86	2.66	2.77	2.80	2.62	2.52
d_6 (Å)	1.87	1.63	1.05	1.83	1.63	1.03
α_1 (deg)	176.9	177.0	176.2	177.7	177.1	175.7
α_2 (deg)	174.3	175.0	174.9	173.5	171.2	174.1

[a]Either NH_3CH_3, mimicking Lys181 (left columns), or a water molecule (right columns), is present in the model system to act as a proton acceptor.

Table 2. Geometric Parameters Obtained from Minimized Structures for Model Systems of the N7 Reaction (Figure 3)

	reactant complex	transition state	product complex
d_1 (Å)	1.82	2.30	3.98
d_2 (Å)	4.94	4.40	5.44
d_3 (Å)	3.12	2.11	1.47
α_1 (deg)	177.4	180.0	176.6

system (i.e., leaving only the reactive water molecule). In that case, no proton transfer is observed yielding a protonated methoxy group in the product state (data not shown).

Energy Profiles. The Gibbs free energies were calculated for all geometries of the optimized structures of all model systems for reactant (left), transition (middle), and product state (right) and are illustrated in Figure 4. Table 3 summarizes all free energies.

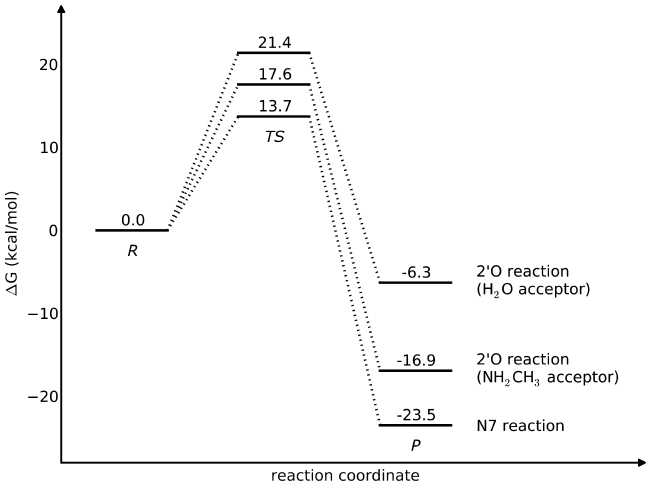

Figure 4. Gibbs free energy profile for reactants, product, and transition state, obtained from DFT calculations for the N7 and the 2′O methyl transfer reaction. For the 2′O reaction, either NH_3CH_3, mimicking Lys181, or a water molecule is present in the model system to act as a proton acceptor.

For both the 2′O as well as the N7 system, the calculations reveal that the reactions are exergonic processes where the product state is energetically significantly lowered compared to the reactant state with an energetically unfavorable transition state in between. The Gibbs free energy difference between product and reactant is −23.5 kcal/mol for the N7 reaction and −16.9 kcal/mol for the catalyzed 2′O reaction. For the transition state, an energy barrier of 13.7 and 17.6 kcal/mol

Table 3. Summary of the Gibbs Free Energies for Reactant, Product, and Transition State, Obtained from Ab Initio Model System Calculations for the N7 and the 2′O Methyl Transfer Reaction[a]

	2′O reaction (NH_2CH_3 proton acceptor)	2′O reaction (H_2O proton acceptor)	N7 reaction
reactant complex	0.0	0.0	0.0
transition state	17.6	21.4	13.7
product complex	−16.9	−6.3	−23.5

[a]For the 2′O reaction, either NH_3CH_3, mimicking Lys181, or a water molecule is present in the model system to act as a proton acceptor.

is observed for N7 and catalyzed 2′O reactions, respectively. From experimentally determined turnover numbers (k_{cat}) for the 2′O reaction, the activation barrier of this reaction can be estimated with transition state theory[29] using the formula $k_{cat} = (k_B T)/h \cdot \exp(-\Delta G^{\ddagger}/(RT))$ where $\Delta G^{\ddagger}$ is the activation barrier, T the temperature, R the universal gas constant, k_B the Boltzmann constant, and h the Planck constant. k_{cat} values have been reported between 2.47×10^{-3} s^{-1} and 3.25×10^{-4} s^{-1} which yield estimated activation barriers in the range 21.0−22.2 kcal/mol.[30,31] Thus, the calculated activation energy barriers are in a similar range indicating that the postulated S_N2-type methyl transfer reaction is energetically feasible. It should be noted that DFT methods are known to generally underestimate barrier heights.[32]

When the uncatalyzed 2′O methyl transfer reaction is compared to the catalyzed one (Table 3 columns 1 and 2), a significant reduction of the product state free energy can be observed in the catalyzed reaction. The product state energy is lowered by 10.6 kcal/mol and the reaction energy barrier is lowered by 3.8 kcal/mol which, based on transition state theory, corresponds to a reaction rate enhancement of ∼600 times.

In summary, for the 2′O reaction, the data suggests the importance of the correct proton acceptor moiety. In the catalyzed reaction, a lysine residue, representing Lys181 in the active site of the protein, acts as a proton acceptor and significantly stabilizes the product state and reduces the activation barrier compared to the reaction in aqueous solution. The N7 methyl transfer reaction, on the other hand, has a significantly lower energy barrier to overcome in aqueous solution and is thus more likely to occur without direct protein interactions. In conclusion, the data agrees well with the mechanistic hypothesis, where the 2′O reaction needs direct involvement of protein residues, whereas the N7 methylation

dx.doi.org/10.1021/jp5028564 | J. Phys. Chem. B XXXX, XXX, XXX−XXX

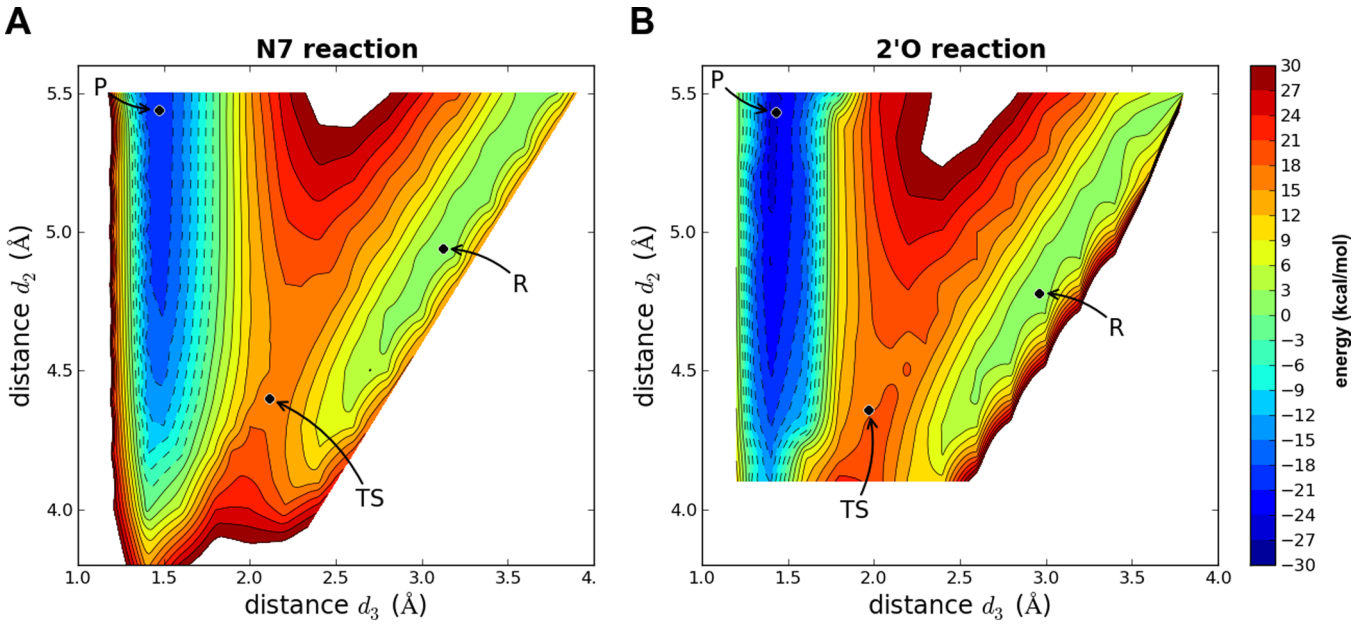

Figure 5. Two dimensional potential energy landscape for model systems of the N7 (A) and the 2′O reaction (B). Energies are shown for two reaction coordinates: (*x*-axis) distance between the acceptor atom and the transferring CH_3 group (d_3); (*y*-axis) distance between the acceptor and the donor atoms (d_2). Reaction coordinates of the fully optimized structures are highlighted with points and labeled with their state.

does not need direct contact with the protein as long as the two reactants are in close proximity.[5]

Energy Landscapes. In the optimized transition state structure a compression of the methyl donor−acceptor distance was observed, as described above. To further characterize the effect of this compression on the activation barrier and to analyze reaction pathways, two-dimensional potential energy landscapes for the model system of the N7 and the 2′O reaction were computed and are displayed in Figure 5. Enthalpies of partially optimized systems are reported, computed on a grid using the following two reaction coordinates: (1) the distance between the acceptor atom and the transferring methyl group (distance d_3 in Figure 3); (2) the distance between the acceptor and the donor atom (distance d_2 in Figure 3).

From this data, a qualitative picture of the reaction process can be obtained. Both reaction coordinates as well as activation barriers of the partially optimized energy landscapes are in good agreement with the fully optimized structures as shown in Figure 5 where the values of the reaction coordinates of the fully optimized structures are indicated with black dots.

For both reactions, two distinct minima were observed which are shallow along d_3: one corresponding to the reactant state with acceptor−methyl group distances above 2.5 Å and an energetically more favored minimum corresponding to the product state with acceptor−methyl group distances around 1.5 Å. The two minima are connected by a saddle point corresponding to the transition state which is more diffuse for the N7 reaction and tighter for the 2′O reaction. When the system is moved along its minimum energy pathway from the reactants through the transition state to the products, the system first compresses where the donor−acceptor distance (d_2) reduces from ∼5.0 Å to ∼4.5 Å and then expands again to its product state with a donor−acceptor distance of ∼5.5 Å. Thus, this compression significantly reduces the activation barrier compared to a direct movement without changing the donor−acceptor distance.

Instead of using an optimized structure for the heavy atoms, the X-ray positions could be employed. However, this is prone to exhibit internal strain as the resolution of a model based on X-ray structures of homologue MTases is limited. Alternatively, further two-dimensional maps could be computed for structures from an MD-sampled ensemble. This has been done successfully for the infrared spectroscopy of CO in myoglobin or for proton transfer reactions.[33,34] However, for two-dimensional PES scans such a calculation would be computational quite prohibitive. Compared to calculations in which the entire structure of ths system is allowed to relax for given values of the reaction coordinates, the approach used in the present work has the advantage to yield an upper estimate for the barrier.

Point Charges. Partial charges obtained from a natural population analysis (NPA)[26] performed on the optimized model structures (see Figure 2) are displayed in Figure 6 using a color gradient from red (−0.8*e*) to green (0.8*e*) and partial charges for substructures of the model systems are summarized in Table 4.

The computed point charges establish that the methyl group is transferred as a cation ($CH_3^{\delta+}$). For both reactions, a redistribution of the charge within the SAM moiety is observed first, when moving from the reactant to the transition state, followed by a charge transfer to the lysine or *N*-methylimidazol moiety for the 2′O and N7 reaction, respectively, when moving from the transition to the product state. For the 2′O reaction, the charge is localized more strongly on the transferred methyl group compared to the N7 reaction, yielding a higher charge on the methyl group both in the transition state and in the product. In comparison, for the N7 reaction, the charge is more evenly distributed among donor, methyl group, and acceptor, yielding a higher charge on SAM and the *N*-methylimidazole moiety in the transition state.

In the product state of the N7 reaction, the charge is located predominantly on the carbon atom at position 2 of the *N*-methylimidazol moiety with a point charge of 0.30*e*, whereas for

dx.doi.org/10.1021/jp5028564 | J. Phys. Chem. B XXXX, XXX, XXX−XXX

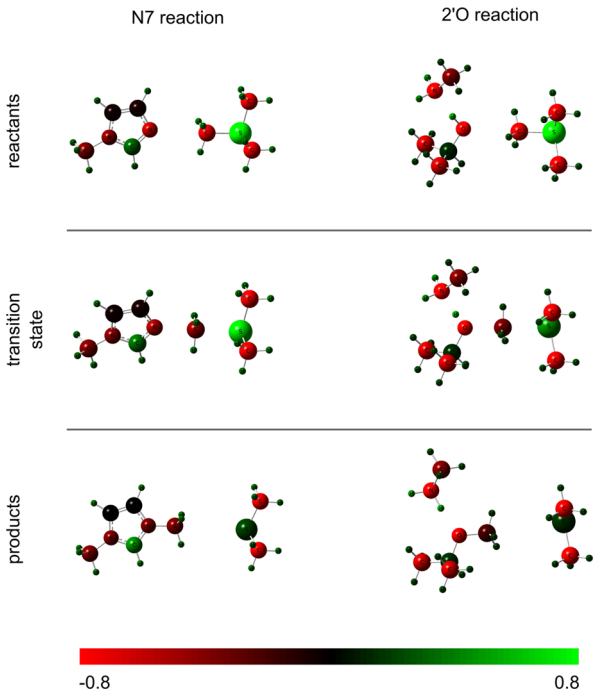

Figure 6. NBO point charges from ab initio calculations mapped onto the model systems for the N7 (left) and the 2′O reaction (right). The color gradient ranges from −0.8 (red) to 0.8*e* (green). Numerical values for substructures are given in Table 4.

the 2′O reaction, the charge is located to a large extent on the proton which was transferred to the model lysine moiety, with a charge of 0.46*e*.

Evidence for a Concerted Mechanism. Methyl transfer reactions to aromatic nitrogen acceptors typically do not need general base catalysis since orienting the nitrogen lone pair toward the SAM methyl group is sufficient. On the contrary, in the case of hydroxyl oxygen acceptors a general base mediates the substitution of a proton by a methyl group where the proton can be abstracted before, during, or after the methyl transfer reaction.[1] For the DENV MTase 2′O reaction the catalytic lysine residue acts as a proton acceptor. However, so far, it is unknown if the methyl transfer and the proton transfer occur as two individual steps or as a single concerted reaction. In a two-step mechanism the catalytic lysine residue deprotonates the 2′-hydroxy group initially. This leads to the formation of a 2′-oxyanion onto which the methyl group is transferred in a subsequent step. In a concerted mechanism on the other hand, the proton is transferred to the catalytic lysine simultaneously to the methyl transfer. Thus, prior to the reaction, the proton acceptor does not deprotonate the 2′-hydroxy group but steers its orientation. NMR experiments indicate that the latter mechanism is operative in the enzymatic reaction of vaccinia virus mRNA cap specific 2′O MTase VP39.[27]

Geometry optimized model structures support a concerted mechanism, as in the reactant and the transition state the proton is still bound to the ribose model compound and only transferred to the proton acceptor in the product state. The distance between the 2′-oxygen atom and the proton (d_4) is 0.99, 1.04, and 1.72 Å for reactants, transition state, and products, respectively.

To confirm this, a linear scan was performed by moving the proton from the 2′O hydroxy group to the Nζ of the lysine model moiety (distance d_6 in Figure 3). During the scan, the methyl group was fixed in the reactant state and thus bound to the SAM model compound. Therefore, the end point of the scan yields a 2′-oxyanion. The energy profile is shown in Figure 7A and the partial charges are summarized in Table 5. The calculations estimate the cost for proton transfer prior to the methyl transfer to ∼10 kcal/mol. The profile increases monotonically and no significant minimum was observed. These findings suggest a concerted mechanism as the oxyanion conformation is not stabilized.

It should be noted that, when the methyl group is moved to its product state, i.e., bound to the ribose moiety, minimization of the structure yields a spontaneous proton transfer with no observable barrier in between. This was confirmed by a linear scan of the proton position when the methyl group is in its product state (Figure 7B). This scan estimates the energy gain for the proton transfer in the product state to ∼20 kcal/mol.

To summarize, these calculations show that the two modeled intermediate states are unstable and thus suggest that the two reactions occur in a concerted fashion where no oxyanion hole is generated but the orientation of the proton acceptor steers the 2′O hydroxy lone pair into the direction of the nucleophilic attack. This is also indicated by the electron density distributions as shown in Figure 8.

Inhibition by SAM Analogues. Analogues of SAM that are stable under physiological conditions and still retain their binding affinity to their target protein have been described in the literature.[35−37] To investigate the effect of such analogues on the methyl transfer reaction and the mechanism of inhibition, we have extended our study to the stable quaternary dimethylammonium analogue of SAM (MeAzaSAM), an isostructural mimic which also carries a positive charge (Figure 1C).

Table 6 shows the Gibbs free energy profiles for optimized structures of the reactant, transition, and product state for the

Table 4. Partial Charges Computed by Natural Bond Orbital Analysis for Substructures of the Model Systems for the 2′O and the N7 Reaction[a]

	2′O reaction					N7 reaction		
	SAH	CH_3	ribose	proton	lysine	SAH	CH_3	guanine
reactant	0.92	0.07	−0.54	0.49	0.05	0.90	0.08	0.01
TS	0.41	0.32	−0.36	0.51	0.12	0.48	0.25	0.27
product	0.01	0.34	−0.29	0.46	0.49	0.01	0.19	0.80

[a]The following substructures were used: (SAH) model of SAM without the reactive methyl group, thus consisting of CH_3SCH_3, (CH_3) reactive methyl group, (ribose) model of the ribose moiety without the reactive methyl group and the proton, (proton) transferred proton, (lysine) model of the lysine side chain without the transferred proton for the 2′O reaction, (guanine) model of the guanine acceptor for the N7 reaction. For different states, the individual chemical moieties are composed differently as indicated by the borders around the table cells.

dx.doi.org/10.1021/jp5028564 | J. Phys. Chem. B XXXX, XXX, XXX−XXX

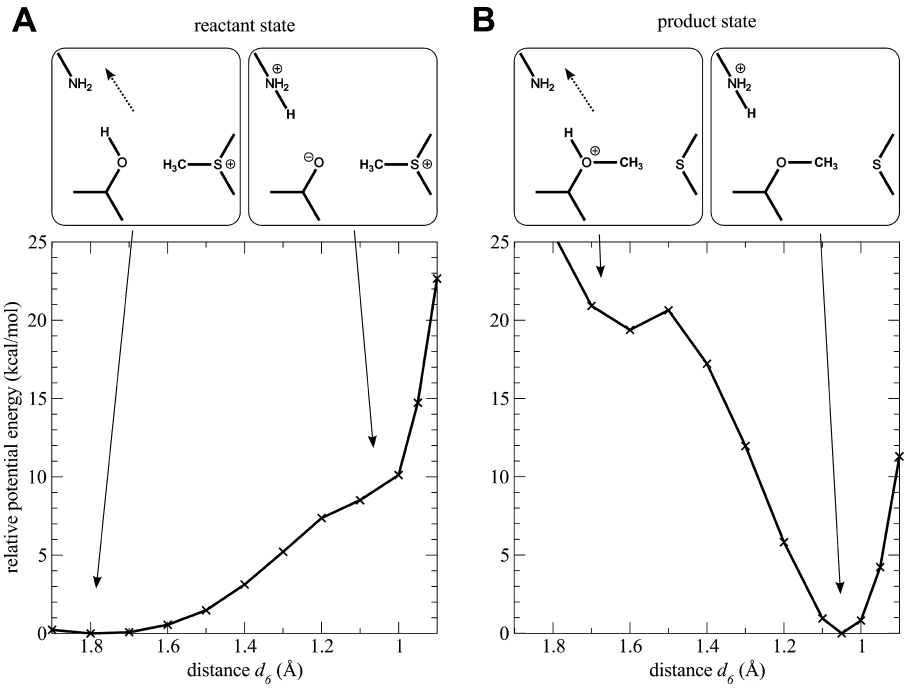

Figure 7. Potential energy curve for the proton transfer obtained by moving the proton from the ribose proton donor (d_6: 1.9 Å) to the lysine proton acceptor (d_6: 1.0 Å). The direction of the scan is indicated with an arrow. (A) System is in the reactant state (methyl group bound to the SAM donor, d_1: 1.8 Å). (B) System is in the product state (methyl group is bound to ribose acceptor, d_1: 4.0 Å).

Table 5. Partial Charges Computed by NBO Analysis for Different States along the Proton Transfer Path (See Figure 7)[a]

	SAH	CH_3	ribose	proton	lysine
		Reactant State			
d_6 = 1.8 Å	0.91	0.08	−0.56	0.50	0.06
d_6 = 1.0 Å	0.90	0.08	−0.91	0.45	0.48
		Product State			
d_6 = 1.6 Å	0.01	0.40	−0.15	0.54	0.21
d_6 = 1.5 Å	0.01	0.34	−0.29	0.46	0.49

[a]The following substructures were used: (SAH) model of SAM without the reactive methyl group, thus consisting of CH_3SCH_3, (CH_3) reactive methyl group, (ribose) model of the ribose moiety without the reactive methyl group and the proton, (proton) transferred proton, and (lysine) model of the lysine side chain without the reactive proton. For different states, the individual chemical moieties are composed differently as indicated by the borders around the table cells.

N7 and the 2′O reaction with the SAM analogue. For both systems, a significantly larger barrier was observed for the methyl transfer reaction with MeAzaSAM (34.0 and 27.2 kcal/mol) compared to the reaction with SAM (17.6 and 13.7 kcal/mol). The overall reactions are endergonic where the product state is energetically higher than the reactant state by 3.3 and 1.3 kcal/mol, respectively. The high activation barriers and the unfavorable product energies clearly indicate that the methyl transfer reaction with MeAzaSAM is unlikely to occur under biologically relevant conditions and that MeAzaSAM could thus be a potential inhibitor of the reactions catalyzed by the dengue MTase.

■ DISCUSSION AND CONCLUSIONS

In this study, we have investigated the two distinct methyl transfer reactions catalyzed by the disease related dengue virus

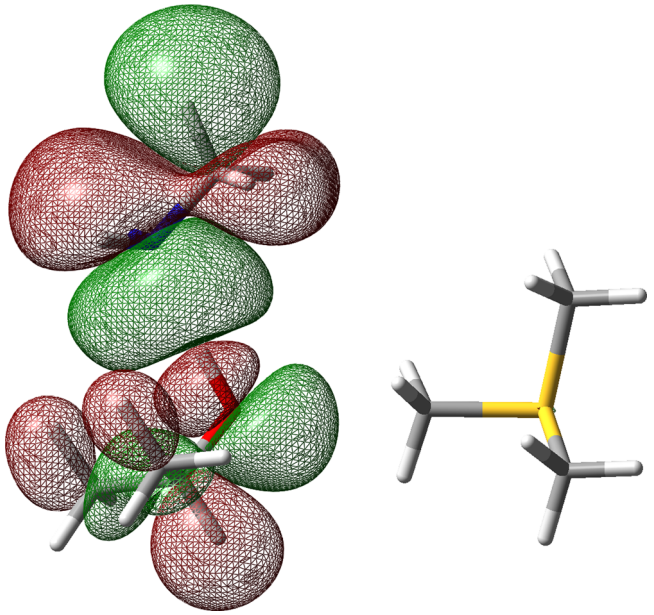

Figure 8. Surface representation of the highest occupied molecular orbital (HOMO) of the reactant geometry for the 2′O reaction. The proton acceptor group steers the lone pair of the 2′ hydroxy group toward the reactive methyl group.

SAM-dependent methyltransferase. Based on DFT calculations on model systems, we have further characterized the underlying chemical reactions. Based on minimized structures of the reactants, the transition state, and the products, we have investigated geometric arrangements, energetics of the reaction, and transfer of charges for both the 2′O and the N7 reactions in detail. The calculations show that the overall reactions are exergonic processes with significant activation barriers. The reactions occur as S_N2-type nucleophilic substitution reactions

dx.doi.org/10.1021/jp5028564 | J. Phys. Chem. B XXXX, XXX, XXX−XXX

Table 6. Gibbs Free Energy Profile for Reactants, Product, and Transition State, Obtained from Ab Initio Model System Calculations for the N7 (Orange) and the 2′O Methyl Transfer Reaction with the Stable SAM Analogue MeAzaSAM

	2′O reaction (NH_2CH_3 proton acceptor)	N7 reaction
reactant complex	0.0	0.0
transition state	34.0	27.2
product complex	3.3	1.3

with linear arrangements, compressed transition states, and a transfer of the methyl group as a cationic species.

For the 2′O reaction, we found that the "protein" environment substantially lowers the activation barrier, mediated by an active site lysine residue, representing Lys181 in the active site of the protein. This lysine residue acts as a proton acceptor during the methyl transfer reaction and stabilizes the transition state as well as the product state compared to the uncatalyzed reaction in aqueous solution.

The overall 2′O reaction is composed of two distinct reactions: a methyl transfer and a proton transfer reaction. Based on geometry optimizations and potential energy scans, we have shown that these two reactions occur in a concerted fashion where during the methyl transfer, the proton is transferred to the proton acceptor. Thus, prior to the reaction, the proton acceptor does not deprotonate the 2′-hydroxy group (no oxyanion hole) but rather steers the orientation of the proton acceptor lone pair.

Furthermore, we have investigated the effect on the reaction and the mechanism of inhibition of stable nitrogen analogues of SAM which have been described in the literature and which were proposed as inhibitors of methyl transfer reactions. Calculations on MeAzaSAM, an isostructural mimic of SAM, show that the overall reactions are endergonic processes with very large activation barriers. These high activation barriers and the unfavorable product energies clearly indicated that the methyl transfer reaction with MeAzaSAM is unlikely to occur under biologically relevant conditions and that this analogue might thus be a viable inhibitor.

Throughout this study the role of dynamics was not included explicitly. One possibility to include such effects would be at the level of mixed quantum mechanics/molecular mechanics simulations.[38,39] Such simulations are, however, computationally very demanding. Alternatively, the quantum mechanical part could be treated at the semiempirical level (e.g., SCC-DFTB[40,41]) or by resorting to adiabatic reactive molecular dynamics simulations.[42−46] This would need to be coupled to enhanced sampling techniques such as umbrella sampling because the barriers involved are high.[47]

AUTHOR INFORMATION

Corresponding Author

*E-mail: m.meuwly@unibas.ch. Phone: +41 (0)61 267 38 21. Fax: +41 (0)61 267 38 55.

Notes

The authors declare no competing financial interest.

ACKNOWLEDGMENTS

The authors would like to thank Dr. Juergen Haas for numerous fruitful discussions. Financial support from the Swiss National Science Foundation (SNF) through grants 200021-117810 (to MM) and the NCCR-MUST (to MM) is gratefully acknowledged.

REFERENCES

(1) Klimasauskas, S.; Lukinavicius, G. *Wiley Encyclopedia of Chemical Biology*; John Wiley and Sons, Inc., 2007.
(2) Cantoni, G. L. Biological Methylation - Selected Aspects. *Annu. Rev. Biochem.* **1975**, *44*, 435−451.
(3) Schubert, H. L.; Blumenthal, R. M.; Cheng, X. D. Many Paths to Methyltransfer: A Chronicle of Convergence. *Trends Biochem. Sci.* **2003**, *28*, 329−335.
(4) Cantoni, G. L. The Nature of the Active Methyl Donor Formed Enzymatically from L-Methionine and Adenosinetriphosphate. *J. Am. Chem. Soc.* **1952**, *74*, 2942−2943.
(5) Fabrega, C.; Hausmann, S.; Shen, V.; Shuman, S.; Lima, C. D. Structure and Mechanism of mRNA cap (guanine-N7) Methyltransferase. *Mol. Cell* **2004**, *13*, 77−89.
(6) Hodel, A. E.; Gershon, P. D.; Quiocho, F. A. Structural Basis for Sequence-Nonspecific Recognition of 5′-Capped mRNA by a Cap-Modifying Enzyme. *Mol. Cell* **1998**, *1*, 443−447.
(7) Hager, J.; Staker, B. L.; Bugl, H.; Jakob, U. Active Site in RrmJ, a Heat Shock-Induced Methyltransferase. *J. Biol. Chem.* **2002**, *277*, 41978−41986.
(8) Copeland, R. A.; Solomon, M. E.; Richon, V. M. Protein Methyltransferases As a Target Class for Drug Discovery. *Nat. Rev. Drug Discuss.* **2009**, *8*, 724−732.
(9) Mannisto, P. T.; Kaakkola, S. Catechol-O-methyltransferase (COMT): Biochemistry, Molecular Biology, Pharmacology, And Clinical Efficacy of the New Selective COMT Inhibitors. *Pharmacol. Rev.* **1999**, *51*, 593−628.
(10) Ferron, F.; Decroly, E.; Selisko, B.; Canard, B. The Viral RNA Capping Machinery As a Target for Antiviral Drugs. *Antivir. Res.* **2012**, *96*, 21−31.
(11) Egloff, M. P.; Benarroch, D.; Selisko, B.; Romette, J. L.; Canard, B. An RNA Cap (Nucleoside-2′-O-)-methyltransferase in the Flavivirus RNA Polymerase NS5: Crystal Structure and Functional Characterization. *EMBO J.* **2002**, *21*, 2757−2768.
(12) Cleaves, G.; Dubin, D. Methylation Stratus of Intracellular Dengue Type 2 40 S RNA. *Virology* **1979**, *96*, 159−165.
(13) Furuichi, Y.; Shatkin, A. J. Viral and Cellular mRNA Capping: Past and Prospects. *Adv. Virol. Res.* **2000**, *55*, 135−184.
(14) Ray, D.; Shah, A.; Tilgner, M.; Guo, Y.; Zhao, Y. W.; Dong, H. P.; Deas, T. S.; Zhou, Y. S.; Li, H. M.; Shi, P. Y. West Nile Virus 5′-Cap Structure Is Formed by Sequential Guanine N-7 and Ribose 2′-O Methylations by Nonstructural Protein 5. *J. Virol.* **2006**, *80*, 8362−8370.
(15) Dong, H. P.; Ren, S. P.; Zhang, B.; Zhou, Y. S.; Puig-Basagoiti, F.; Li, H. M.; Shi, P. Y. West Nile Virus Methyltransferase Catalyzes Two Methylations of the Viral Rna Cap through a Substrate-Repositioning Mechanism. *J. Virol.* **2008**, *82*, 4295−4307.
(16) Dong, H. P.; Zhang, B.; Shi, P. Y. Flavivirus Methyltransferase: A Novel Antiviral Target. *Antivir. Res.* **2008**, *80*, 1−10.
(17) Bollati, M.; et al. Structure and Functionality in Flavivirus NS-Proteins: Perspectives for Drug Design. *Antivir. Res.* **2010**, *87*, 125−148.
(18) Zhou, Y. S.; Ray, D.; Zhao, Y. W.; Dong, H. P.; Ren, S. P.; Li, Z.; Guo, Y.; Bernard, K. A.; Shi, P. Y.; Li, H. M. Structure and Function of Flavivirus NS5 Methyltransferase. *J. Virol.* **2007**, *81*, 3891−3903.
(19) Egloff, M. P.; Decroly, E.; Malet, H.; Selisko, B.; Benarroch, D.; Ferron, F.; Canard, B. Structural and Functional Analysis of Methylation and 5′-RNA Sequence Requirements of Short Capped RNAs by the Methyltransferase Domain of Dengue Virus NS5. *J. Mol. Biol.* **2007**, *372*, 723−736.
(20) Frisch, M. J. et al. *Gaussian 03*, rev D.02; Gaussian, Inc., Wallingford, CT, 2004,.
(21) Becke, A. Density-Functional Thermochemistry. III. The Role Of Exact Exchange. *J. Chem. Phys.* **1993**, *7*, 5648−5652.

(22) Ochterski, J.; Petersson, G.; Montgomery, J. A Complete Basis Set Model Chemistry. V. Extensions to Six or More Heavy Atoms. *J. Chem. Phys.* **1996**, *104*, 2598−2619.
(23) Castejon, H.; Wiberg, K. Solvent Effects on Methyl Transfer Reactions. 1. The Menshutkin Reaction. *J. Am. Chem. Soc.* **1999**, *121*, 2139−2146.
(24) Cossi, M.; Rega, N.; Scalmani, G.; Barone, V. Energies, Structures, and Electronic Properties of Molecules in Solution with the C-PCM solvation Model. *J. Comput. Chem.* **2003**, *24*, 669−681.
(25) Peng, C. Y.; Schlegel, H. B. Combining Synchronous Transit and Quasi-Newton Methods to Find Transition-States. *Isr. J. Chem.* **1993**, *33*, 449−454.
(26) Reed, A. E.; Weinstock, R. B.; Weinhold, F. Natural Population Analysis. *J. Chem. Phys.* **1985**, *83*, 735−746.
(27) Li, C.; Xia, Y.; Gao, X.; Gershon, P. D. Mechanism of RNA 2′-O-Methylation: Evidence that the Catalytic Lysine Acts to Steer Rather than Deprotonate the Target Nucleophile. *Biochemistry* **2004**, *43*, 5680−5687.
(28) Li, C.; Gershon, P. D. pK(a) of the mRNA Cap-Specific 2′-O-Methyltransferase Catalytic Lysine by HSQC NMR Detection of a Two-Carbon Probe. *Biochemistry* **2006**, *45*, 907−917.
(29) Eyring, H. The Activated Complex in Chemical Reactions. *J. Chem. Phys.* **1935**, *3*, 107−115.
(30) Lim, S. P.; Wen, D. Y.; Yap, T. L.; Yan, C. K.; Lescar, J.; Vasudevan, S. G. A Scintillation Proximity Assay for Dengue Virus NS5 2′-O-methyltransferase-kinetic and Inhibition Analyses. *Antivir. Res.* **2008**, *80*, 360−369.
(31) Selisko, B.; Peyrane, F. F.; Canard, B.; Alvarez, K.; Decroly, E. Biochemical Characterization of the (Nucleoside-2′O)-methyltransferase Activity of Dengue Virus Protein NS5 Using Purified Capped RNA Oligonucleotides (7Me)GpppAC(n) and GpppAC(n). *J. Gen. Vir.* **2010**, *91*, 112−121.
(32) Zhao, Y.; Gonzalez-Garcia, N.; Truhlar, D. G. Benchmark Database of Barrier Heights for Heavy Atom Transfer, Nucleophilic Substitution, Association, and Unimolecular Reactions and Its Use to Test Theoretical Methods. *J. Phys. Chem. A* **2005**, *109*, 2012−2018.
(33) Meuwly, M. *ChemPhysChem* **2006**, *7*, 2061.
(34) Lutz, S.; Tubert-Brohman, I.; Yang, Y.; Meuwly, M. Water-Assisted Proton Transfer in Ferredoxin I. *J. Biol. Chem.* **2011**, *286*, 23679−23687.
(35) Thompson, M. J.; Mekhalfia, A.; Jakeman, D. L.; Phillips, S. E. V.; Phillips, K.; Porter, J.; Blackburn, G. M. Homochiral Synthesis of an Aza Analogue of S-Adenosyl-L-methionine (AdoMet) and Its Binding to the E-Coli Methionine Repressor Protein (MetJ). *Chem. Commun.* **1996**, 791−792.
(36) Thompson, M. J.; Mekhalfia, A.; Hornby, D. P.; Blackburn, G. M. Synthesis of Two Stable Nitrogen Analogues of S-adenosyl-L-methionine. *J. Org. Chem.* **1999**, *64*, 7467−7473.
(37) Joce, C.; Caryl, J.; Stockley, P. G.; Warriner, S.; Nelson, A. Identification of Stable S-Adenosylmethionine (SAM) Analogues Derivatised with Bioorthogonal Tags: Effect of Ligands on the Affinity of the E. coli Methionine Repressor, MetJ, for Its Operator DNA. *Org. Biomol. Chem.* **2009**, *7*, 635−638.
(38) Warshel, A.; Levitt, M. Theoretical Studies Of Enzymic Reactions - Dielectric, Electrostatic And Steric Stabilization Of Carbonium-Ion In Reaction Of Lysozyme. *J. Mol. Biol.* **1976**, *103*, 227−249.
(39) Field, M.; Bash, P.; Karplus, M. A Combined Quantum-Mechanical And Molecular Mechanical Potential For Molecular-Dynamics Simulations. *J. Comput. Chem.* **1990**, *11*, 700−733.
(40) Elstner, M.; Porezag, D.; Jungnickel, G.; Elsner, J.; Haugk, M.; Frauenheim, T.; Suhai, S.; Seifert, G. Self-Consistent-Charge Density-Functional Tight-Binding Method for Simulations of Complex Materials Properties. *Phys. Rev. B* **1998**, *58*, 7260−7268.
(41) Cui, Q.; Elstner, M.; Kaxiras, E.; Frauenheim, T.; Karplus, M. A QM/MM Implementation of the Self-Consistent Charge Density Functional Tight Binding (SCC-DFTB) Method. *J. Phys. Chem. B* **2001**, *105*, 569−585.
(42) Nutt, D. R.; Meuwly, M. Studying Reactive Processes with Classical Dynamics: Rebinding Dynamics in MbNO. *Biophys. J.* **2006**, *90*, 1191−1201.
(43) Danielsson, J.; Meuwly, M. Atomistic Simulation of Adiabatic Reactive Processes Based on Multi-State Potential Energy Surfaces. *J. Chem. Theor. Comput.* **2008**, *4*, 1083−1093.
(44) Mishra, S.; Meuwly, M. Atomistic Simulation of NO Dioxygenation in Group I Truncated Hemoglobin. *J. Am. Chem. Soc.* **2010**, *132*, 2968−2982.
(45) Nienhaus, K.; Lutz, S.; Meuwly, M.; Nienhaus, G. U. Reaction-Pathway Selection in the Structural Dynamics of a Heme Protein. *Chem. Commun.* **2013**, *19*, 3558−3562.
(46) Nagy, T.; Yosa, J.; Meuwly, M. Multi-State Adiabatic Reactive Molecular Dynamics. *J. Chem. Theor. Comput.* **2014**, *10* (4), 1366−1375.
(47) Torrie, G. M.; Valleau, J. Non-Physical Sampling Distributions In Monte-Carlo Free-Energy Estimation - Umbrella Sampling. *J. Comput. Phys.* **1977**, *23*, 187−199.